HAL
open science

Large Enhancement of Ferromagnetism under a Collective Strong Coupling of YBCO Nanoparticles

Anoop Thomas, Eloise Devaux, Kalaivanan Nagarajan, Guillaume Rogez, Marcus Seidel, Fanny Richard, Cyriaque Genet, Marc Drillon, Thomas Ebbesen

To cite this version:

Anoop Thomas, Eloise Devaux, Kalaivanan Nagarajan, Guillaume Rogez, Marcus Seidel, et al.. Large Enhancement of Ferromagnetism under a Collective Strong Coupling of YBCO Nanoparticles. Nano Letters, 2021, 21 (10), pp.4365-4370. 10.1021/acs.nanolett.1c00973 . hal-03343102

HAL Id: hal-03343102

https://hal.science/hal-03343102v1

Submitted on 13 Sep 2021

HAL is a multi-disciplinary open access archive for the deposit and dissemination of scientific research documents, whether they are published or not. The documents may come from teaching and research institutions in France or abroad, or from public or private research centers.

L'archive ouverte pluridisciplinaire **HAL**, est destinée au dépôt et à la diffusion de documents scientifiques de niveau recherche, publiés ou non, émanant des établissements d'enseignement et de recherche français ou étrangers, des laboratoires publics ou privés.

NANO LETTERS

pubs.acs.org/NanoLett

Letter

Large Enhancement of Ferromagnetism under a Collective Strong Coupling of YBCO Nanoparticles

Anoop Thomas, Eloise Devaux, Kalaivanan Nagarajan, Guillaume Rogez, Marcus Seidel, Fanny Richard, Cyriaque Genet, Marc Drillon,* and Thomas W. Ebbesen*

Cite This: https://doi.org/10.1021/acs.nanolett.1c00973

Read Online

ACCESS | Metrics & More | Article Recommendations | Supporting Information

ABSTRACT: Light−Matter strong coupling in the vacuum limit has been shown, over the past decade, to enhance material properties. Oxide nanoparticles are known to exhibit weak ferromagnetism due to vacancies in the lattice. Here we report the 700-fold enhancement of the ferromagnetism of $YBa_2Cu_3O_{7-x}$ nanoparticles under a cooperative strong coupling at room temperature. The magnetic moment reaches 0.90 μ_B/mol, and with such a high value, it competes with $YBa_2Cu_3O_{7-x}$ superconductivity at low temperatures. This strong ferromagnetism at room temperature suggest that strong coupling is a new tool for the development of next-generation magnetic and spintronic nanodevices.

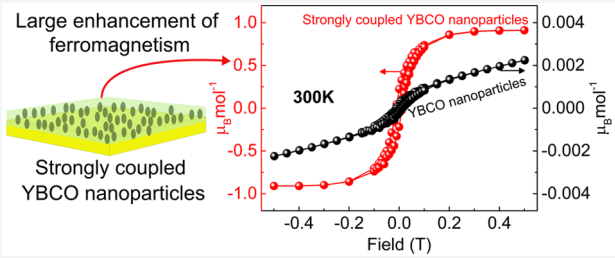

KEYWORDS: *strong coupling, ferromagnetism, superconductivity, vibration*

■ INTRODUCTION

Over the past decade, strong coupling has proven to be a promising way to modify and control properties of materials such as charge and energy transport,[1−13] superconductivity,[14−16] work function,[17] nonlinear optics.[18−21] and chemical reactivity.[22] In strong coupling, the material is typically placed in the confined electromagnetic field of a cavity or a surface plasmon tuned to be in resonance with a material transition. Under the right conditions, new hybrid light−matter states appear, called polaritonic states such as P+ and P−, as shown in Figure 1, modifying the ladder of energy levels of the material. Furthermore, this occurs even in the dark due to the interaction between the zero-point energy fluctuations of both the optical mode and the material.

Strong coupling is facilitated by collective coupling, whereby a large number N of oscillators such as molecules couple to a single optical mode.[23] This enhances the Rabi splitting $\hbar\Omega_R$, the energy that separates the polaritonic states P+ and P−, as $\sqrt{N}$. In addition, $N - 1$ so-called dark states (DS) are formed. P+, P−, and DS are all collective states, delocalized over the optical mode volume (Figure 1A).

In the course of studying the effects of a strong coupling of phonons on superconducting microcrystalline powders, we found that, while the critical temperature Tc of Rb_3C_{60} is increased by 30 to 45 K, that of the $YBa_2Cu_3O_{7-x}$ oxide (YBCO) decreased from 92 to 86 K.[14] While the Rb_3C_{60} is a phonon-based superconductor and therefore the change in Tc could be rationalized, the change in YBCO was not expected, since the underlying pairing mechanism is not described by Bardeen-Cooper-Schrieffer (BCS) theory,[24] and is believed to involve both strong electron correlations and phonon-mediated interactions between electrons.[25,26] In trying to understand the change in YBCO using a superconducting quantum interference device (SQUID) magnetometer, we found that, in parallel to the superconductivity, another property was being modified by strong coupling, namely, the magnetic response.

YBCO bulk material is a well-known spin singlet superconductor that exhibits in the normal state antiferromagnetic short-range correlations. However, for nanoparticle (NP) samples, unexpected room-temperature ferromagnetism, with a well-defined hysteresis cycle, has been reported, which is believed to be related to the presence of oxygen vacancies created at the surface of NPs.[27−33] Such a behavior has given rise to a huge number of studies of oxides, nitrides, or sulfides, which are expected to be nonmagnetic but exhibit room-temperature ferromagnetism when they are dispersed at the nanoscale. The net moment is usually very low and, accordingly, can be attributed to magnetic impurities, but several reliable experimental and density functional theory (DFT)-based theoretical studies conclude that it is likely intrinsic and due to oxygen vacancies.[28,34] For instance, a direct magnetic imaging of the nonmagnetic $SrTiO_3$ fully

Received: March 10, 2021
Revised: April 16, 2021

Downloaded via UNIV STRASBOURG on May 5, 2021 at 08:53:38 (UTC).
See https://pubs.acs.org/sharingguidelines for options on how to legitimately share published articles.

ACS Publications

© XXXX The Authors. Published byAmerican Chemical Society

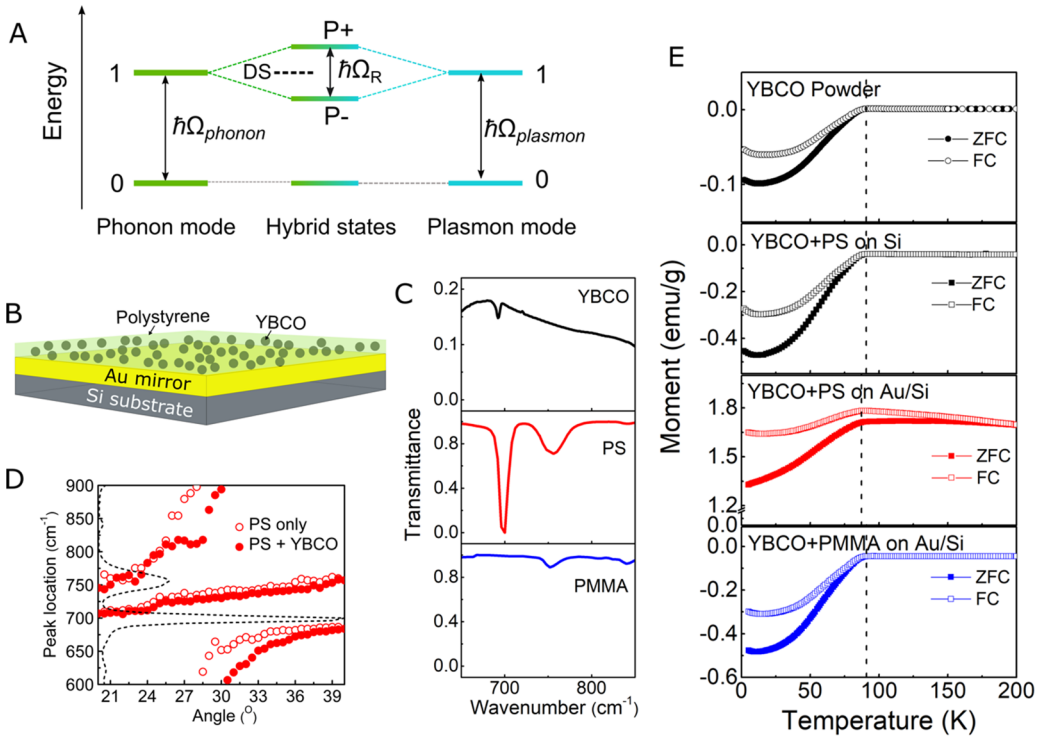

Figure 1. (A) Schematic illustration of the strong coupling (cooperative) between the phonon mode of the YBCO and the surface plasmon mode of the Au film. The hybrid states P+ and P− are separated by the Rabi splitting energy, and the DS are represented by the black dashed lines. (B) Illustration of the cooperatively strongly coupled YBCO nanoparticles embedded in the polymer matrix. The YBCO-containing PS is spin-coated onto the Au (10 nm) film sputtered on the Si window. The PS matrix is shown in green, and the embedded YBCO NPs are shown as dark circles. (C) FTIR transmission spectra of the YBCO particles (black curve), PS (red curve), and PMMA (blue curve). (D) Dispersion curves, measured by attenuated total reflectance FTIR spectroscopy, showing the cooperative strong coupling of the surface plasmon mode with the PS vibration at 697 cm^{-1}, which overlaps with the YBCO phonon mode. The empty red circles represent the strong coupling for PS alone, and the solid circles show the PS+YBCO mixture. The PS transmission spectrum is shown by the black dashed curve. (E) Temperature-dependent magnetization of the YBCO powder (black circles), film of YBCO+PS on Si (black squares), strongly coupled YBCO+PS on Au/Si (red squares), and cooperatively off-resonant YBCO+PMMA on Au/Si (blue squares) in the ZFC (filled squares and circles) and 100 Oe FC (empty squares and circles) modes in the temperature range of 4−200 K. The onset of superconducting transition (Tc) was determined from the intersection point of the polynomial fits on the ZFC and FC curves. The bare film features a Tc of 92 K, while it is shifted to 87 K for the strongly coupled YBCO as shown by the dashed lines in the respective panels.

supports this assumption.[31] By using ultrahigh-resolution photoemission electron microscopy (PEEM), it was shown that ferromagnetic nanodomains develop at the oxygen-deficient surface of the sample, even for temperatures well above 300 K, confirming the existence of an intrinsic ferromagnetism.

Here we report that, under a collective strong coupling, this ferromagnetism is enhanced by 2−3 orders of magnitude to the point that it even can perturb the superconductivity and lower the Tc of YBCO. There are several parameters that are critical to observe such an enhancement in the ferromagnetism. They can be rationalized by the collective states that favor spin alignment and increase the magnetic domain size.

■ RESULTS

Since YBCO has phonon modes that are weakly absorbing, the best way to strongly couple this material to the surface plasmon mode of Au films is to use the cooperative coupling technique illustrated in Figure 1B. In this approach, the material to be coupled is placed in a polymer matrix that has a strong vibrational band that overlaps one of the YBCO phonon bands. The polymer vibrational band is strongly coupled and transfers the coupling property to the material thru a cooperative process described in detail elsewhere.[35,36] This technique works well for molecular solutions and fine powders as in the present study, where the average particle size is ∼200 nm (Figure S1A,B). This cooperative regime generates extended states that favors a long-distance interaction within and between particles.

The samples were prepared using commercial YBCO powder purchased from Can Superconductors. The X-ray diffraction (XRD) pattern (see Figure S2) shows that the YBCO has, as expected, the orthorhombic structure (i.e., the 123 phase) and that there is a very small amount of the green phase Y_2BaCuO_5. Note that this extra phase does not affect the magnetic properties nor the superconducting transition of $YBa_2Cu_3O_{7-x}$ at 92 K. The YBCO was further ground in a mortar before mixing it with a polymer solution (either polystyrene (PS) or poly(methyl methacrylate) (PMMA)). The mixed solution was then spin-coated on a sputtered Au film deposited on a high-purity Si substrate (the preparation conditions are important, see the Supporting Information for more details). The Au film supports the surface plasmons that couple to the material vibrational band (Figure 1B). The Fourier transform infrared (FTIR) data for the powder used in this study is shown in Figure 1C together with those of the PS and PMMA. We couple cooperatively the 697 cm^{-1} phonon band of YBCO, using the overlap with the vibrational mode of

https://doi.org/10.1021/acs.nanolett.1c00973
Nano Lett. XXXX, XXX, XXX−XXX

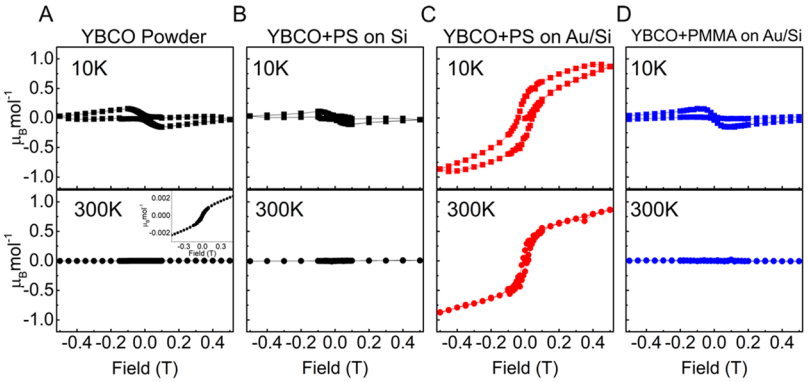

Figure 2. $M(H)$ curves of YBCO at 10 and 300 K. (A) YBCO powder; inset in the bottom panel gives an enlargement of the $M(H)$ at 300 K showing the weakly ferromagnetic character of the powder; (B) thin film of YBCO+PS on Si; (C) strongly coupled thin film of YBCO+PS on Au/Si; and (D) cooperatively off-resonant thin film of YBCO+PMMA on Au/Si. All the curves, except the powder (A), were corrected for the diamagnetic signal of the Si substrate.

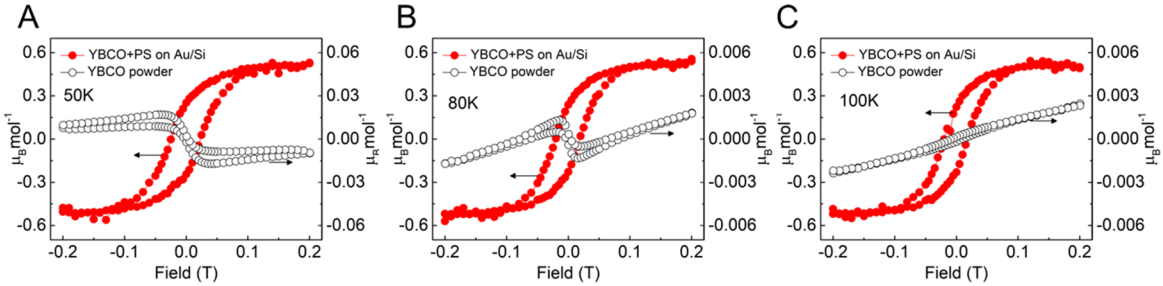

Figure 3. (A−C) Comparison of the $M(H)$ curves of the strongly coupled YBCO (YBCO+PS on Au/Si; red filled circles) and YBCO powder (black empty circles) at temperatures near the superconducting transition of YBCO. (A) 50, (B) 80, and (C) 100 K.

PS (Figure 1C). The corresponding dispersion curve of the strongly coupled sample with surface plasmon is shown in Figure 1D. PMMA, which has no bands that overlap with YBCO phonon mode, was used as a reference. The Tc of YBCO only shifts to lower temperatures when the sample is cooperatively coupled using PS, as shown in Figure 1E. In addition to the Tc shift, notice the positive magnetic moment in this condition and the difference between the field-cooled (FC) and zero-field-cooled (ZFC) curves above Tc, due to the appearance of the enhanced ferromagnetism under a cooperative strong coupling.

Note that the IR spectrum of YBCO is very dependent on the origin of the sample and how the sample was prepared. For instance, the YBCO peak at 697 cm^{-1} that we couple in these experiments has been attributed to an apical oxygen stretching mode of the crystal structure,[37,38] but it could also arise from the small amount of carbon retention during the fabrication of YBCO, which generates a barium carbonate ($BaCO_3$) type of environment. The latter results from the incorporation of C in the YBCO structure and is mainly associated with the surface as shown in several studies[39,40] and disappears upon a high-temperature annealing in an inert atmosphere. X-ray photoelectron spectroscopy (XPS) confirms that the YBCO in this study contains a small amount of $BaCO_3$ (see Figure S4). Since the Tc of our bare powder is 92 K, it indicates that nevertheless the carbon content is less than 0.04%, according to the literature.[41]

Figure 2 compares the magnetic response of the YBCO at 10 and 300 K for various conditions: (A) the original powder, (B) the YBCO dispersed in PS on Si substrate, (C) on Au-coated Si substrate, and (D) the same as the latter for YBCO dispersed in PMMA. The $M(H)$ curves at 10 K, for samples A, B, and D, exhibit the typical butterfly-like behavior of the superconducting YBCO phase. The minimum of magnetization, at 0.1 T, is the critical field beyond which the field penetrates the sample. It agrees well with previous findings, which range between 100 and 200 mT depending on the material.[42,43] In turn, when using PS as polymer matrix (Figure 2C), a striking change of $M(H)$ occurs, since a ferromagnetic behavior takes place with a saturation value of ∼0.90 μB/mol and a coercive field of 40 mT at 10 K. At 300 K, the pure YBCO powder (sample A) exhibits a paramagnetic behavior with a weak ferromagnetic component detected at low field, but that is much weaker than for the strongly coupled sample (YBCO in PS matrix on Au/Si). Note that the uncoupled samples B and D show at 300 K very similar $M(H)$ variations to that of powder sample A.

What is most striking in these experiments is that the magnetic moment is enhanced by a factor of 700 under the collective strong coupling at room temperature. The observed magnetic moment of 0.90 μ_B/mol is very large and cannot be explained by assuming that it originates only from anion vacancies at the surface of YBCO NPs, since less than 1% of the YBCO unit cells are at the surface. As a result, the contribution of inner NPs oxygen vacancies must be considered. Furthermore, it is not realistic to explain the ferromagnetic contribution at room temperature by the presence of NPs metallic impurities, since their size would have to be several tens of nanometers to remain magnetic at such temperatures. Accordingly, they would be detected by energy-dispersive X-ray analysis (EDAX) (Figure S1C), XRD

https://doi.org/10.1021/acs.nanolett.1c00973
Nano Lett. XXXX, XXX, XXX−XXX

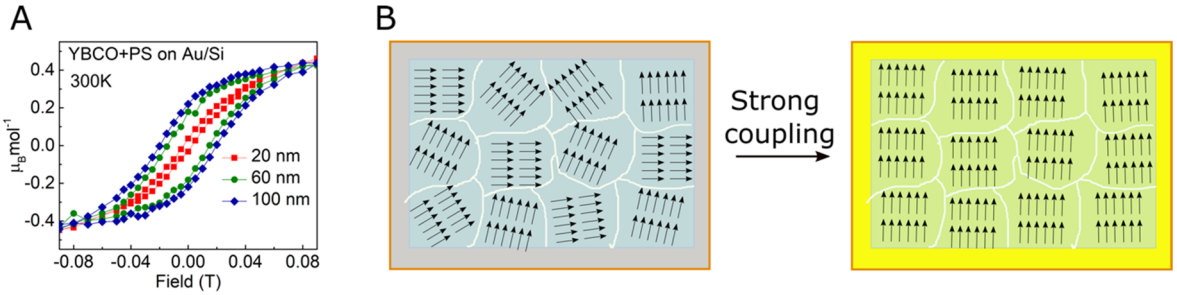

Figure 4. (A) $M(H)$ curves of YBCO at 300 K for varying Au thickness: 20 nm (red squares), 60 nm (green circles), and 100 nm (blue diamonds). (B) A cartoon of the domain structure of the polymer matrix containing YBCO on Si with the magnetic spins in each domain oriented differently and the possible alignment of the magnetic spins under strong coupling resulting in the enhanced ferromagnetism.

(Figure S2), and X-ray photoelectron spectroscopy (XPS) (Figure S4, S5), contrary to our findings.

When the same YBCO is dispersed in PMMA on the Au surface, no enhancement of the magnetism is detectable, as expected, since the cooperative coupling is not possible for this polymer confirming the key role of strong coupling in generating the ferromagnetic enhancement.

The plots of Figure 3 illustrate the striking change of magnetic behavior between uncoupled (powder) and strongly coupled YBCO samples for three different temperatures. While the powder sample shows a significant change of $M(H)$ above Tc, the strongly coupled one is dominated by a ferromagnetic-like behavior whatever the temperature. At 80 K, namely, just below the Tc, it can be observed that a small ferromagnetic component already exists in the powder sample, which competes with a superconducting state, and that this component is multiplied by at least 2 orders of magnitude in the strongly coupled system.

Since the strong coupling involves the surface plasmons of the Au film, we also studied the effect of the Au film thickness as shown in Figure 4. The hysteretic behavior and, in particular, the net moment of the magnetization increases with the Au thickness and saturates above 100 nm. This is related to the quality of the optical response of the Au film, which is known to improve in this thickness range.[44] It confirms the role of the strong-coupling-induced hybridization between the phonons and the surface plasmons in enhancing the magnetic response.

■ DISCUSSION AND CONCLUSION

Similarly to dilute ferromagnetic oxides,[28,45,46] shallow donor electrons, related to oxygen vacancies, form magnetic polarons that mediate magnetic ordering. However, both the very high ordering temperature, above 300 K, and the significant magnetic moment (0.90 μ_B/mol) make such a model unrealistic to explain our results. Note that this also rules out the effect of impurities made of transition-metal oxide or pure-metal nanoparticles. As a result, surface states alone can no longer explain the magnetic behavior and a model based on the effect of a strong coupling between plasmons, generated in the bulk YBCO compound, and spin carriers must be considered.

Ferromagnetic domains already exist in pure nanosized YBCO powder, due to oxygen vacancies, and it has been well-established that they can coexist with superconductivity when the magnetic field is less than a threshold value H^*, beyond which Cooper pairs are destroyed.[29,30] These magnetic domains would be related to a hopping mechanism of the unpaired electrons like that reported for dilute magnetic semiconductors. Such a mechanism is well-known in mixed-valence systems, where the transfer of an excess electron between neighboring sites is allowed only for parallel spin configurations of the valence electrons.[47−49] Then, ferromagnetism is promoted. The magnitude of the coupling being given by the transfer integral (on the order of 10^3 K), such that very high ordering temperatures are expected, as observed for YBCO NP powders (T_{Curie} ~800 K).[28]

Under a strong coupling, the behavior of YBCO NPs exhibits a striking variation as evidenced by the magnetic moment that is boosted by orders of magnitude and remains so even at room temperature. Then, the competition with the superconducting states below Tc appears crucial because of the antagonism between both properties. A description of the behavior necessitates introducing the coupling between electronic states and phonon modes of the network. At a very low temperature, the growth of magnetic domains is most likely collective and related to the breaking of Cooper pairs for an increasing external field. The delocalization of the unpaired electrons then promotes nanodomains to line up in the field direction, which in turn reinforces existing ferromagnetic domains. In this process, coherent phonon modes induced by the strong coupling play a major role. In turn, when the field decreases below H^*, the spins condense into Cooper pairs progressively so as to form the superconducting nanodomains, but this recombination is limited by the internal field of the ferromagnetic domains.

At high temperatures, only ferromagnetic domains remain. The variation of the net moment at 300 K, from 0.037 to 0.22 μB/mol for Au thickness ranging from 20 to 100 nm, confirms the key role of plasmon resonance in the growth of magnetic domains. Furthermore, the value of the magnetic moment points out that the inner spins participate in the magnetic ordering and is not limited to the NPs surface.

Finally, the existence of ferromagnetism at room temperature makes such systems suitable for the development of next-generation spintronic nanodevices. Usually, the limitation in NP magnetic materials stems from the fact that they are characterized by a low-temperature blocking temperature. Strong coupling of NP materials such as YBCO may be a promising solution to get around this limitation. Our results, together with the recent theoretical prediction of enhanced ferroelectric phase transition,[50] further broadens the appeal of strong coupling with the vacuum field to engineer material properties.

https://doi.org/10.1021/acs.nanolett.1c00973
Nano Lett. XXXX, XXX, XXX−XXX

■ ASSOCIATED CONTENT

Supporting Information

The Supporting Information is available free of charge at https://pubs.acs.org/doi/10.1021/acs.nanolett.1c00973.

Experimental methods, FT-IR, SEM, EDAX, XRD, and XPS characterization of YBCO powder (PDF)

■ AUTHOR INFORMATION

Corresponding Authors

Marc Drillon − *University of Strasbourg, CNRS, IPCMS, 67034 Strasbourg, France*; Email: marc.drillon@ipcms.unistra.fr

Thomas W. Ebbesen − *University of Strasbourg, CNRS, ISIS, 67000 Strasbourg, France*; orcid.org/0000-0002-3999-1636; Email: ebbesen@unistra.fr

Authors

Anoop Thomas − *University of Strasbourg, CNRS, ISIS, 67000 Strasbourg, France*

Eloise Devaux − *University of Strasbourg, CNRS, ISIS, 67000 Strasbourg, France*

Kalaivanan Nagarajan − *University of Strasbourg, CNRS, ISIS, 67000 Strasbourg, France*

Guillaume Rogez − *University of Strasbourg, CNRS, IPCMS, 67034 Strasbourg, France*

Marcus Seidel − *University of Strasbourg, CNRS, ISIS, 67000 Strasbourg, France*

Fanny Richard − *University of Strasbourg, CNRS, ISIS, 67000 Strasbourg, France*

Cyriaque Genet − *University of Strasbourg, CNRS, ISIS, 67000 Strasbourg, France*; orcid.org/0000-0003-0672-7406

Complete contact information is available at: https://pubs.acs.org/10.1021/acs.nanolett.1c00973

Author Contributions

The manuscript was written through contributions of all authors. All authors have given approval to the final version of the manuscript.

Notes

The authors declare no competing financial interest.

■ ACKNOWLEDGMENTS

We thank S. Reisner and T. Adler (QD Europe) for their help in SQUID magnetometer measurements. We acknowledge support of the International Center for Frontier Research in Chemistry (icFRC), the ANR Equipex Union (ANR-10-EQPX-52-01), the Labex NIE Projects (ANR-11-LABX-0058 NIE), CSC (ANR-10-LABX-0026 CSC), and USIAS within the Investissement d'Avenir program ANR-10-IDEX-0002-02, the ERC (Project No. 788482 MOLUSC) and QuantERA project RouTe. M.S. acknowledges support from the Marie Skłodowska-Curie actions of the European Commission (Project No. 753228, PlaN).

■ REFERENCES

(1) Orgiu, E.; George, J.; Hutchison, J. A.; Devaux, E.; Dayen, J. F.; Doudin, B.; Stellacci, F.; Genet, C.; Schachenmayer, J.; Genes, C.; Pupillo, G.; Samorì, P.; Ebbesen, T. W. Conductivity in Organic Semiconductors Hybridized with the Vacuum Field. *Nat. Mater.* **2015**, *14*, 1123−1129.

(2) Hagenmüller, D.; Schachenmayer, J.; Schütz, S.; Genes, C.; Pupillo, G. Cavity-Enhanced Transport of Charge. *Phys. Rev. Lett.* **2017**, *119*, 223601.

(3) Bartolo, N.; Ciuti, C. Vacuum-Dressed Cavity Magneto-Transport of a Two-Dimensional Electron Gas. *Phys. Rev. B: Condens. Matter Mater. Phys.* **2018**, *98*, 205301.

(4) Paravicini-Bagliani, G. L.; Appugliese, F.; Richter, E.; Valmorra, F.; Keller, J.; Beck, M.; Bartolo, N.; Rössler, C.; Ihn, T.; Ensslin, K.; Ciuti, C.; Scalari, G.; Faist, J. Magneto-Transport Controlled by Landau Polariton States. *Nat. Phys.* **2019**, *15*, 186−190.

(5) Krainova, N.; Grede, A. J.; Tsokkou, D.; Banerji, N.; Giebink, N. C. Polaron Photoconductivity in the Weak and Strong Light-Matter Coupling Regime. *Phys. Rev. Lett.* **2020**, *124*, 177401.

(6) Nagarajan, K.; George, J.; Thomas, A.; Devaux, E.; Chervy, T.; Azzini, S.; Joseph, K.; Jouaiti, A.; Hosseini, M. W.; Kumar, A.; Genet, C.; Bartolo, N.; Ciuti, C.; Ebbesen, T. W. Conductivity and Photoconductivity of a p-Type organic Semiconductor under Ultra-Strong Coupling. *ACS Nano* **2020**, *14*, 10219−10225.

(7) Gonzalez-Ballestero, C.; Feist, J.; Moreno, E.; Garcia-Vidal, F. J. Harvesting Excitons through Plasmonic Strong Coupling. *Phys. Rev. B: Condens. Matter Mater. Phys.* **2015**, *92*, 121402.

(8) Coles, D. M.; Somaschi, N.; Michetti, P.; Clark, C.; Lagoudakis, P. G.; Savvidis, P. G.; Lidzey, D. G. Polariton-Mediated Energy Transfer between Organic Dyes in a Strongly Coupled Optical Microcavity. *Nat. Mater.* **2014**, *13*, 712−719.

(9) Zhong, X.; Chervy, T.; Zhang, L.; Thomas, A.; George, J.; Genet, C.; Hutchison, J. A.; Ebbesen, T. W. Energy Transfer between Spatially Separated Entangled Molecules. *Angew. Chem., Int. Ed.* **2017**, *56*, 9034−9038.

(10) Akulov, K.; Bochman, D.; Golombek, A.; Schwartz, T. Long-Distance Resonant Energy Transfer Mediated by Hybrid Plasmonic−Photonic Modes. *J. Phys. Chem. C* **2018**, *122*, 15853−15860.

(11) Feist, J.; Garcia-Vidal, F. J. Extraordinary Exciton Conductance Induced by Strong Coupling. *Phys. Rev. Lett.* **2015**, *114*, 196402.

(12) Schachenmayer, J.; Genes, C.; Tignone, E.; Pupillo, G. Cavity-Enhanced Transport of Excitons. *Phys. Rev. Lett.* **2015**, *114*, 196403.

(13) Rozenman, G. G.; Akulov, K.; Golombek, A.; Schwartz, T. Long-Range Transport of Organic Exciton-Polaritons Revealed by Ultrafast Microscopy. *ACS Photonics* **2018**, *5*, 105−110.

(14) Thomas, A.; Devaux, E.; Nagarajan, K.; Chervy, T.; Seidel, M.; Hagenmüller, D.; Schütz, S.; Schachenmayer, J.; Genet, C.; Pupillo, G.; Ebbesen, T. W. *Exploring Superconductivity under Strong Coupling with the Vacuum Electromagnetic Field*. 2019, *arXiv* [cond-mat.supr-con] https://arxiv.org/abs/1911.01459 (Accessed 2021-04-15).

(15) Sentef, M. A.; Ruggenthaler, M.; Rubio, A. Cavity Quantum-Electrodynamical Polaritonically Enhanced Electron-Phonon Coupling and Its Influence on Superconductivity. *Sci. Adv.* **2018**, *4*, eaau6969.

(16) Schlawin, F.; Cavalleri, A.; Jaksch, D. Cavity-Mediated Electron-Photon Superconductivity. *Phys. Rev. Lett.* **2019**, *122*, 133602.

(17) Hutchison, J. A.; Liscio, A.; Schwartz, T.; Canaguier-Durand, A.; Genet, C.; Palermo, V.; Samori, P.; Ebbesen, T. W. Tuning the Work-Function via Strong Coupling. *Adv. Mater.* **2013**, *25*, 2481−2485.

(18) Chervy, T.; Xu, J.; Duan, Y.; Wang, C.; Mager, L.; Frerejean, M.; Münninghoff, J. A. W.; Tinnemans, P.; Hutchison, J. A.; Genet, C.; Rowan, A. E.; Rasing, T.; Ebbesen, T. W. High-Efficiency Second-Harmonic Generation from Hybrid Light-Matter States. *Nano Lett.* **2016**, *16*, 7352−7356.

(19) Barachati, F.; Simon, J.; Getmanenko, Y. A.; Barlow, S.; Marder, S. R.; Kéna-Cohen, S. Tunable Third-Harmonic Generation from Polaritons in the Ultrastrong Coupling Regime. *ACS Photonics* **2018**, *5*, 119−125.

(20) Liu, B.; Crescimanno, M.; Twieg, R. J.; Singer, K. D. Dispersion of Third-Harmonic Generation in Organic Cavity Polaritons. *Adv. Opt. Mater.* **2019**, *7*, 1801682.

(21) Wang, K.; Seidel, M.; Nagarajan, K.; Chervy, T.; Genet, C.; Ebbesen, T. W. Large Optical Nonlinearity Enhancement under

Electronic Strong Coupling. *Nat. Commun.* **2021**, DOI: 10.1038/s41467-021-21739-7.
(22) Ebbesen, T. W. Hybrid Light−Matter States in a Molecular and Material Science Perspective. *Acc. Chem. Res.* **2016**, *49*, 2403−2412.
(23) Törmä, P.; Barnes, W. L. Strong Coupling between Surface Plasmon Polaritons and Emitters: a Review. *Rep. Prog. Phys.* **2015**, *78*, 013901.
(24) Bardeen, J.; Cooper, L. N.; Schrieffer, J. R. Theory of Superconductivity. *Phys. Rev.* **1957**, *108*, 1175−1204.
(25) Zhao, G.; Hunt, M. B.; Keller, H.; Müller, K. A. Evidence for Polaronic Supercarriers in the Copper Oxide Superconductors La 2−x Sr x CuO 4. *Nature* **1997**, *385*, 236−239.
(26) Schneider, T.; Keller, H. Universal Trends in Extreme Type-II Superconductors. *Phys. Rev. Lett.* **1992**, *69*, 3374−3377.
(27) Shipra; Gomathi, A.; Sundaresan, A.; Rao, C. N. R. Room-Temperature Ferromagnetism in Nanoparticles of Superconducting Materials. *Solid State Commun.* **2007**, *142*, 685−688.
(28) Sundaresan, A.; Rao, C. N. R. Ferromagnetism as a Universal Feature of Inorganic Nanoparticles. *Nano Today* **2009**, *4*, 96−106.
(29) Hasanain, S. K.; Akhtar, N.; Mumtaz, A. Particle Size Dependence of the Superconductivity and Ferromagnetism in YBCO Nanoparticles. *J. Nanopart. Res.* **2011**, *13*, 1953−1960.
(30) Gasmi, M.; Khene, S.; Fillion, G. Coexistence of Superconductivity and Ferromagnetism in Nanosized YBCO Powders. *J. Phys. Chem. Solids* **2013**, *74*, 1414−1418.
(31) Taniuchi, T.; Motoyui, Y.; Morozumi, K.; Rödel, T. C.; Fortuna, F.; Santander-Syro, A. F.; Shin, S. Imaging of Room-Temperature Ferromagnetic Nano-Domains at the Surface of a Non-Magnetic Oxide. *Nat. Commun.* **2016**, *7*, 11781.
(32) Das Pemmaraju, C.; Sanvito, S. Ferromagnetism driven by intrinsic point defects in HfO2. *Phys. Rev. Lett.* **2005**, *94*, 217205.
(33) Zhang, Z. H.; Wang, X.; Xu, J. B.; Muller, S.; Ronning, C.; Li, Q. Evidence of intrinsic ferromagnetism in individual dilute magnetic semiconducting nanostructures. *Nat. Nanotechnol.* **2009**, *4*, 523−527.
(34) Sharma, P.; Gupta, A.; Rao, K. V.; Owens, F. J.; Sharma, R.; Ahuja, R.; Guillen, J. M. O.; Johansson, B.; Gehring, G. A. Ferromagnetism above room temperature in bulk and transparent thin films of Mn-doped ZnO. *Nat. Mater.* **2003**, *2*, 673−677.
(35) Lather, J.; Bhatt, P.; Thomas, A.; Ebbesen, T. W.; George, J. Cavity Catalysis by Cooperative Vibrational Strong Coupling of Reactant and Solvent Molecules. *Angew. Chem., Int. Ed.* **2019**, *58*, 10635−10638.
(36) Schütz, S.; Schachenmayer, J.; Hagenmüller, D.; Brennen, G. K.; Volz, T.; Sandoghdar, V.; Ebbesen, T. W.; Genes, C.; Pupillo, G. Ensemble-Induced Strong Light-Matter Coupling of a Single Quantum Emitter. *Phys. Rev. Lett.* **2020**, *124*, 113602.
(37) Arai, M.; Yamada, K.; Hidaka, Y.; Itoh, S.; Bowden, Z. A.; Taylor, A. D.; Endoh, Y. Anomaly of Phonon State of Superconducting $YBa_2Cu_3O_7$ Studied by Inelastic Neutron Scattering. *Phys. Rev. Lett.* **1992**, *69*, 359−362.
(38) Calvani, P.; Capizzi, M.; Lupi, S.; Balestrino, G. Infrared Active Vibrational Modes Strongly Coupled to Carriers in High-Tc Superconductors. *Europhys. Lett. EPL* **1995**, *31*, 473−478.
(39) Shaw, T. M.; Dimos, D.; Batson, P. E.; Schrott, A. G.; Clarke, D. R.; Duncombe, P. R. Carbon Retention in $YBa_2Cu_3O_{7-\delta}$ and Its Effect on the Superconducting Transition. *J. Mater. Res.* **1990**, *5*, 1176−1184.
(40) Wang, J.; Monot, I.; Hervieu, M.; Provost, J.; Desgardin, G. Evidence of Carbon Retention in Ceramics and Its Effect on the Superconducting Properties. *Supercond. Sci. Technol.* **1996**, *9*, 69−75.
(41) Masuda, Y.; Ogawa, R.; Kawate, Y.; Matsubara, K.; Tateishi, T.; Sakka, S. The Effect of Residual Carbon on the Superconducting Properties of $YBa_2Cu_3O_{7-x}$ Powders. *J. Mater. Res.* **1993**, *8*, 693−698.
(42) Chen, D.-X.; Goldfarb, R. B.; Cross, R. W.; Sanchez, A. Surface barrier and lower critical field in $YBa_2Cu_3O_{7-d}$ superconductors. *Phys. Rev. B: Condens. Matter Mater. Phys.* **1993**, *48*, 6426−6430.
(43) Buntar, V.; Riccò, M.; Cristofolini, L.; Weber, H. W.; Bolzoni, F. Critical Fields of the Superconducting Fullerene $RbCs_2C_{60}$. *Phys. Rev. B: Condens. Matter Mater. Phys.* **1995**, *52*, 4432−4437.
(44) Fontana, E. Thickness Optimization of Metal Films for the Development of Surface-Plasmon-Based Sensors for Nonabsorbing Media. *Appl. Opt.* **2006**, *45*, 7632−7642.
(45) Venkatesan, M.; Fitzgerald, C. B.; Coey, J. M. D. Unexpected Magnetism in a Dielectric Oxide. *Nature* **2004**, *430*, 630−630.
(46) Hong, N. H.; Sakai, J.; Poirot, N.; Brizé, V. Room-Temperature Ferromagnetism Observed in Undoped Semiconducting and Insulating Oxide Thin Films. *Phys. Rev. B: Condens. Matter Mater. Phys.* **2006**, *73*, 132404.
(47) Anderson, P. W.; Hasegawa, H. Considerations on Double Exchange. *Phys. Rev.* **1955**, *100*, 675−681.
(48) Sanchez, C.; Livage, J.; Launay, J. P.; Fournier, M.; Jeannin, Y. Electron Delocalization in Mixed-Valence Molybdenum Polyanions. *J. Am. Chem. Soc.* **1982**, *104*, 3194−3202.
(49) Drillon, M.; Pourroy, G.; Darriet, J. Electronic and Vibronic Coupling in a Mixed-Valence Dimeric Unit d^1-d^2, Magnetic Aspects. *Chem. Phys.* **1984**, *88*, 27−37.
(50) Ashida, Y.; İmamoğlu, A.; Faist, J.; Jaksch, D.; Cavalleri, A.; Demler, E. Quantum Electrodynamic Control of Matter: Cavity-Enhanced Ferroelectric Phase Transition. *Phys. Rev. X* **2020**, *10*, 041027.

https://doi.org/10.1021/acs.nanolett.1c00973
Nano Lett. XXXX, XXX, XXX−XXX